Detailed exploration of the endothelium: parameterization of flow-mediated dilation through principal component analysis

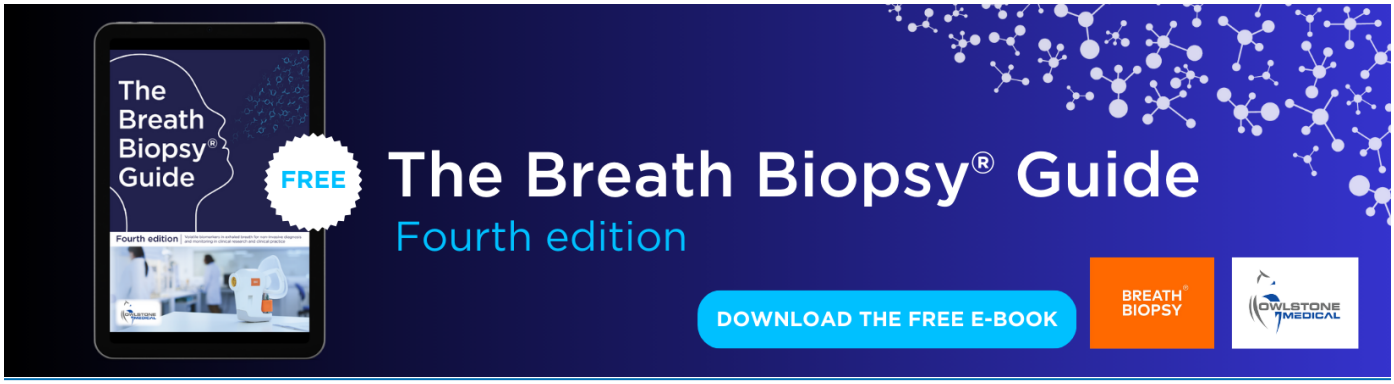

Physiol. Meas. **28** (2007) 301–320 doi:10.1088/0967-3334/28/3/006

Detailed exploration of the endothelium: parameterization of flow-mediated dilation through principal component analysis

Martin Laclaustra[1], Alejandro F Frangi[2], Daniel Garcia[2], Loïc Boisrobert[2], Andres G Frangi[1] and Isaac Pascual[1]

[1] Unit of Cardiovascular Research, University Clinical Hospital Lozano Blesa, Aragon Institute of Health Sciences, Avda. San Juan Bosco, 15, E-50009 Zaragoza, Spain
[2] Computational Imaging Lab, Department of Technology, Pompeu Fabra University, Passeig de Circumval.lació, 8, E-08003 Barcelona, Spain

E-mail: martin.laclaustra@unizar.es and alejandro.frangi@upf.edu

Received 28 May 2006, accepted for publication 25 January 2007
Published 23 February 2007
Online at stacks.iop.org/PM/28/301

Abstract

Endothelial dysfunction is associated with cardiovascular diseases and their risk factors (CVRF), and flow-mediated dilation (FMD) is increasingly used to explore it. In this test, artery diameter changes after post-ischaemic hyperaemia are classically quantified using maximum peak vasodilation (FMDc). To obtain more detailed descriptors of FMD we applied principal component analysis (PCA) to diameter–time curves (absolute), vasodilation–time curves (relative) and blood-velocity–time curves. Furthermore, combined PCA of vessel size and blood-velocity curves allowed exploring links between flow and dilation. Vessel diameter data for PCA (post-ischaemic: 140 s) were acquired from brachial ultrasound image sequences of 173 healthy male subjects using a computerized technique previously reported by our team based on image registration (Frangi *et al* 2003 *IEEE Trans. Med. Imaging* **22** 1458). PCA provides a set of axes (called eigenmodes) that captures the underlying variation present in a database of waveforms so that the first few eigenmodes retain most of the variation. These eigenmodes can be used to synthesize each waveform analysed by means of only a few parameters, as well as potentially any signal of the same type derived from tests of new patients. The eigenmodes obtained seemed related to visual features of the waveform of the FMD process. Subsequently, we used eigenmodes to parameterize our data. Most of the main parameters (13 out of 15) correlated with FMDc. Furthermore, not all parameters correlated with the same CVRF tested, that is, serum lipids (i.e., high LDL-c associated with slow vessel return to a baseline, while low HDL-c associated with a lower vasodilation in response to similar velocity stimulus), thus suggesting that this parameterization allows a more detailed and factored description of the process than FMDc.

Keywords: flow-mediated dilation, cardiovascular disease risk factors, principal component analysis, endothelial function, brachial ultrasound, diagnostic techniques

1. Introduction

Flow-mediated dilation (FMD) has become a common means of assessing endothelial function through using the endothelial response to changes in shear stress (Corretti *et al* 2002, Teragawa *et al* 2001, Cooke *et al* 1991, Sinoway *et al* 1989). In the test, an increased blood flow entails an increase in shear stress, which itself results in a release of nitric oxide. This further triggers the relaxation of smooth muscle cells in the arterial wall, which finally produces arterial dilation. With a diseased endothelium, vasodilation is lower or non-existent as one or more steps of this physiological pathway fail (Moncada and Higgs 1993).

Endothelial dysfunction has been reported to be linked to various cardiovascular risk factors (CVRF) such as hypertension, smoking or unfavourable serum lipids levels (Vita and Keaney 2002, Faulx *et al* 2003, Widlansky *et al* 2003, Gokce *et al* 2003). It also seems to be a precursor of more manifest symptoms and it may be considered itself a potentially modifiable CVRF. Biomarkers of endothelial dysfunction can be valuable for early and late risk assessment as well as for patient monitoring during treatment.

Among the different diagnostic approaches to evaluate endothelial health, FMD has become popular because it is a non-invasive technique. Moreover, B-mode ultrasonography (US) is an inexpensive option for evaluating the vasodilation response (Celermajer *et al* 1992). However, complementary computerized image analysis techniques are still necessary to achieve automation, accuracy and objectivity of the test (Corretti *et al* 2002). These are particularly required when FMD data are used in large clinical trials, or in mechanistic studies on arterial disease and its progression.

FMD is quantified with the peak dilation diameter after hyperaemia, relative to the baseline diameter. Both diameters are not easy to extract directly from visual inspection of the ultrasonographic image sequences. Computerized analysis of the ultrasound sequence, however, automatically yields time series of vessel size from which clinically relevant information can be inferred. Despite a decrease in peak vasodilation having been associated with the presence of CVRF (like hypercholesterolemia (Celermajer *et al* 1992), smoking (Celermajer *et al* 1993a), hyperhomocysteinemia (Celermajer *et al* 1993b), etc), this classic quantification is performed by relying only on two points on the dilation-time waveform, baseline and peak, and does not exploit the entire time course present in the signal from which richer information might be extracted.

How to quantify the interplay between arterial dilation response and haemodynamic changes remains another unsolved problem, given that some of the processes involved in the shear stress-induced dilation are still unknown. Arterial wall shear stress is considered to be the primary stimulus for flow-mediated dilation. It has been shown that FMD is linearly proportional to peak hyperaemic wall shear stress, the latter being related to average blood flow and average arterial diameter (Silber *et al* 2001). Moreover, it may be misleading to derive the aforementioned FMD indices without considering, in the flow signal, the magnitude and shape of the stimulus that provokes the dilation. It seems natural to take this dependence into account when comparing FMD indices in populations of subjects with large variations in the post-ischaemic hyperaemic response.

A quantitative analysis of shear stress and vasodilation and their interdependence is therefore important in order to identify the relationship among the response to shear stress, basal diameter, and hyperaemic flow response, which are all interwoven into the FMD process.

In this paper, we propose the use of principal component analysis (PCA) in order to obtain a global and combined parameterization of FMD and blood velocity (as a surrogate of shear stress) signals that characterizes the waveforms' morphology. FMD and velocity signals were obtained using the registration-based algorithm of Frangi *et al* (2003) and an edge-detection algorithm similar to that presented by Tschirren *et al* (2001), respectively. The usefulness of the proposed parameterization, which renders information consistent with but richer than classic FMD indices, is demonstrated by analysing the correlation between PCA-based indices and other clinical variables (some CVRF) in 173 subjects. The results are compared to those correlations obtained using the classic FMD index.

This paper is organized as follows. In section 2, the source of clinical data is detailed, including the description of the FMD protocol and the population of subjects under study. Section 3 describes the proposed parameterization of FMD signals based on principal component analysis. Section 4 presents the results of the actual PCA and highlights the potential of this new parameterization by studying its connections to classic FMD indices and some CVRF. Subsequently, in section 5, all results are discussed, with conclusions drawn in section 6. In the appendix appears the detailed description of the computerized image pre-processing that provides diameter and velocity signals.

2. Methods: experimental setting and subject population

2.1. Image database and experimental set-up: clinical considerations for the FMD test

A database of ultrasound image sequences was acquired at the University Clinical Hospital Lozano Blesa (Zaragoza, Spain) using a Sonos 4500 ultrasound system (Philips Medical Systems, Andover, MA, USA) in harmonic fusion mode with a 5.5–7.5 MHz trapezoidal multi-frequency probe. Longitudinal bi-dimensional images of the arteries were obtained. Pulsed Doppler was used to visualize Doppler blood velocity spectral waveforms simultaneously on screen, acquired from a 1 mm sample volume in the centre of the artery, with the Doppler beam aligned at approximately 70° with respect to the vessel axis. End-diastolic images synchronous with electrocardiogram R wave were held on the echographic screen and these still images along with the Doppler blood velocity spectral waveforms were subsequently captured by a computer at a rate of 1 frame per second. Images were digitized at a resolution of 768 × 576 pixels. Each sequence consists of approximately 1200 frames for a period of about 20 min.

The experimental set-up was performed as described by Corretti *et al* (2002). Briefly, the FMD tests were performed as follows. An ischaemia was induced in the forearm using a pneumatic cuff distal to the probe. When the cuff was released, a post-ischaemic hyperaemia occurred. Flow-mediated dilation is the vasodilation response to hyperaemia. Five temporal phases of the standard test can be distinguished in each sequence.

Rest state: initial rest state preceding any action performed on the patient.

Distal Ischaemia: inflation of the cuff for 5 min. Motion artefacts provoked by cuff activity often lead to imaging differences between pre-ischaemic and post-ischaemic period.

Flow-mediated dilation: response to reactive hyperaemia. At the beginning of this phase, and coincidental to the cuff release, it is usual to note important undesirable motions of the patient's artery with respect to the ultrasound probe. This phase is the essential one for recovering information on endothelial function.

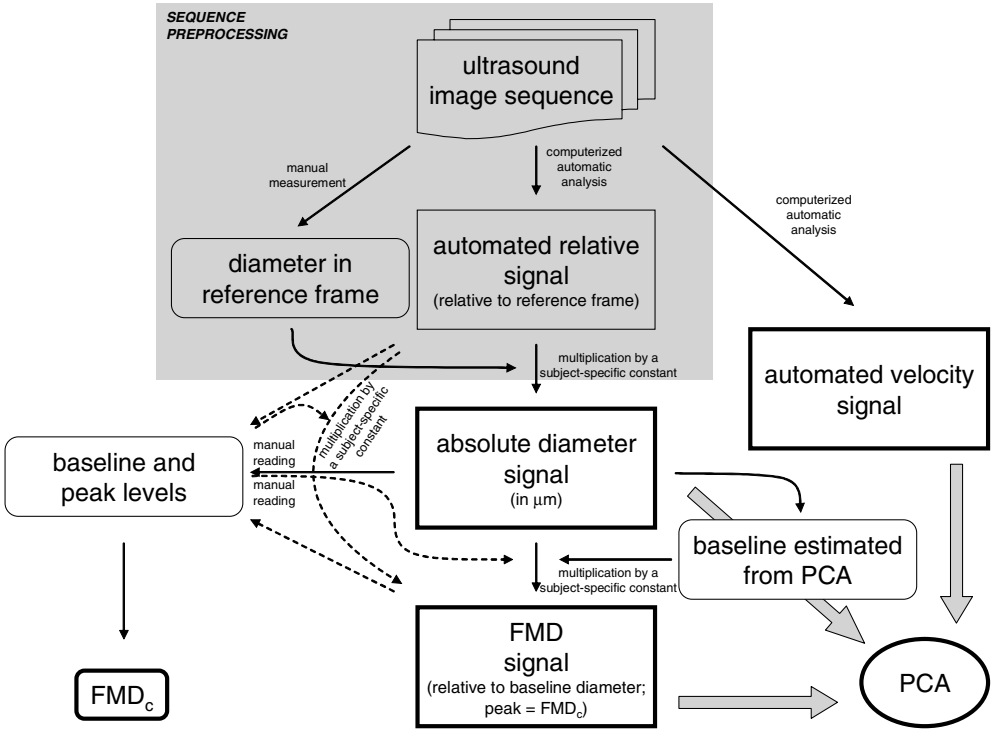

Figure 1. Generation of signals to be analysed from each FMD test (bold-face boxes). The grey box designates pre-processing (explained in the appendix) to obtain the basic initial signals: diameter signal and velocity signal. Discontinuous lines denote alternative ways (not used in this work) to obtain the signals and readings. PCA can be performed irrespectively of how the signals are obtained. The processes outside the grey box are explained in section 3.

Post-FMD rest state: the artery diameter returns to a steady state. This rest state does not necessarily have to coincide with the previous baseline (Corretti *et al* 2002).

Nitroglycerine-mediated dilation: response to sublingual supply of a fixed dose of this chemical vasodilator (8 min after cuff release).

Basically, parameters measured in FMD tests identify vessel diameter changes and haemodynamics changes over time. We used computerized methods (Frangi *et al* 2003) on each test to obtain two data time series that represent absolute diameters (diameter signal) and blood velocities (velocity signal) respectively. See the appendix and figure 1 for details about these methods.

2.2. Sample population

Male volunteers of the Spanish Army (age range: 32–41 years), as part of the AGEMZA Study (a national cohort study of cardiovascular risk factors in young adults) (Casasnovas *et al* 1992, Laclaustra-Gimeno *et al* 2006), underwent FMD tests. The study includes subjects with quite a wide range of clinical profiles (body weight: 62.3–111.8 kg; body mass index—BMI: 20.59–35.36 kg m^{-2}; hypertension: 9%; normal to mildly unfavourable lipid levels, with average total cholesterol and triglycerides: 207.5 mg dl^{-1} and 116.8 mg dl^{-1} respectively; smokers: 21.6%). Total cholesterol, triglycerides and high density lipoprotein

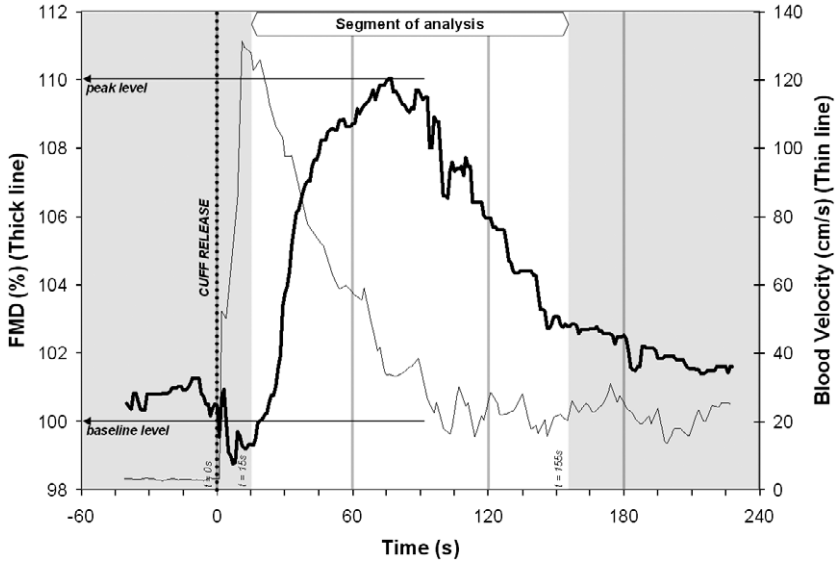

Figure 2. Definition of the segment for PCA (white area). *X*-axis represents time in seconds from cuff release. *Y*-axis represents FMD (bold-face line) and blood velocity (plain line). The segment begins in a zone free from artefacts 15 s after cuff release and has a duration of 140 s. Classic FMD can be obtained by visually reading the baseline and peak levels in the waveforms.

cholesterol (HDL-Cholesterol) analyses were performed using standard enzymatic laboratory techniques. Low density lipoprotein cholesterol (LDL-Cholesterol) levels were calculated using the Friedewald formula (Roberts 1988) in subjects whose triglycerides levels were less than 400 mg dl^{-1}. A total of 173 suitable tests (waveforms free from artefacts) could be utilized after automated processing.

3. Methods: parameterization of FMD and velocity signals

3.1. Initial data

We defined several signals from each test for principal component analysis: the diameter signal that represents absolute vessel diameters; the FMD signal that represents vasodilation values and is expressed as a percentage with respect to a baseline diameter (a 100% value where the artery is not dilated with respect to the baseline diameter); and the velocity signal that represents blood velocities.

Instantaneous diameter and instantaneous blood velocity are continuous biological signals. Nevertheless, we were interested in end-diastolic diameter and average blood velocity across the cardiac cycle, which are discrete signals that take a value for each heart beat. We synchronously sampled these two signals at a rate of 1 Hz to get isochronous simultaneous signals. This sampling was performed when capturing the ultrasound machine images with the computer at a rate of 1 frame per second (see section 2.1).

The FMD signal can be calculated from the diameter signal by dividing the latter by the baseline level that can be manually or automatically obtained from the diameter waveform itself (see figures 1 and 2). To calculate the FMD signal in our case, the baseline level was obtained automatically with a procedure derived from the PCA of the diameter signal, which we describe below (see section 3.4 and figure 1). This level therefore varies from test to test. As such, the scaling factor is a random variable with its own variability, which, in addition, is

not fully independent of the degree of vasodilation (Silber *et al* 2005). Hence, FMD signal and diameter signal deserve an individual analysis because one of them (diameter signal) includes the diameter variance across subjects, which is covariant with the FMD phenomenon. On the one hand, analysis of FMD signal provides insights into the dilation process in accordance with the usual current parameterization (see section 3.2). On the other hand, analysis of diameter signal takes into account intrinsic diameter variability and its association with the dynamics of the vasodilation process. Thus, both signals capture complementary information.

We analysed the velocity signal instead of shear stress or blood flow signals because calculation of the latter includes convoluting blood velocity and diameter signals, and that convolution compromises the independence of both signals in subsequent combined statistical analysis of shear stress or flow and vasodilation.

Focusing on the clinically relevant part of the test (FMD phase), a segment of the signals with a duration of 140 s starting 15 s after cuff release was extracted for PCA (figure 2). This segment was defined to have sufficient duration to capture the main features of the FMD process. The first 15 s were excluded because of the presence of motion artefacts yielding noisy data (see section 2.1).

3.2. Classic parameterization

Relevant information about the endothelium is thought to be found in the arterial diameter changes that follow an intense flow stimulus. Flow information is disregarded and only diameter change is used to measure FMD. Classic FMD (FMD_c) is calculated according to the expression

$$FMD_c = \frac{\Phi_{max} - \Phi_{baseline}}{\Phi_{baseline}} \times 100\% \tag{1}$$

where Φ_{max} and $\Phi_{baseline}$ are maximal and baseline arterial diameters, respectively. The average FMD_c of healthy subjects has a value around 5%, and it takes place about 60 s after release of the cuff (Hardie *et al* 1997).

Equation (1) is valid for any signal related to diameter (in the case of the FMD waveform, values are expressed as percentages of the baseline diameter, and their maximum value is exactly FMD_c allowing direct readings without calculations). To get FMD_c manually, the baseline level was visually read from the diameter waveform, in a region free from artefacts just after cuff release, and the maximum was also identified. Some authors (Celermajer *et al* 1992) use an average of the rest state phase as the baseline level. In our case, the baseline level is read just before the FMD phenomenon to ensure comparison with PCA results, which are determined entirely from the FMD phase. Besides, we observed an acceptable agreement between this level and that of the rest state; when discordances were present, most of the time, these were due to undesirable movements during the test and not to physiological changes. Thus, we avoided artefacts and increased consistency with our choice.

3.3. Global parameterization using PCA

In order to make a global parameterization of the FMD process we propose the use of principal component analysis (PCA) (Jolliffe 2002). PCA is a statistical tool that analyses multidimensional data by determining the dominant axes of variation according to a maximum variance subspace principle. The central idea of principal component analysis (PCA) is to decompose a given signal by projecting it onto a set of basis vectors, each one oriented along a different axis. The signal can then be reconstructed from a linear combination of these basis vectors weighted by the projection coefficients.

The principal components can therefore be compared to the amplitudes of the harmonic functions in a Fourier series. The main difference between Fourier decomposition and decomposition into principal components lies in the set of basis vectors. While in Fourier decomposition the form of the basis vectors is independent of the data to be decomposed (i.e., they are fixed harmonic functions), the basis vectors in principal component analysis are estimated from a database of signals.

PCA computes a set of basis vectors such that the projection coefficients of the data constitute a set of variables, which are uncorrelated and ordered such that the first few retain most of the variation present in all the original variables. Thus, the orientation of the axes depends on the signal variability within the database, capturing the underlying 'principal components' of that variability. Obviously, this assumes that the database used is representative of the phenomenon under analysis. In mathematical terms, PCA is equivalent to an eigenanalysis of the data covariance matrix; therefore, PCA axes (represented by the basis vectors) are often called eigenmodes (or principal components).

We performed PCA on five different datasets: individual PCA of diameter, FMD and velocity waveform segments yielded *EigenD*, *EigenFMD* and *EigenV* modes; combined PCA of each of the data segments of vessel size (diameter and FMD signals) and velocity data segments yielded *EigenDV* and *EigenFMDV*. Individual PCA provided a global parameterization of the different waveforms, while combined PCA gave insight into the relationship between dilation and flow.

The signals analysed as a combined set were merged as follows. For each test, the information on vessel size and blood velocity was combined by concatenation of data segments from the diameter–velocity and FMD–velocity data. As the units and range of both signals were different, each set of segments was normalized using robust estimators before performing the concatenation. For each type of signal (diameter, FMD and velocity), the 10% trimmed mean and the mean absolute deviation of all segments in the set were computed. These robust estimators were used to normalize the data of each signal type, allowing the concatenation of data segments, which are measured in the same units (Z scores) after normalization.

The directions of the PCA axes are arbitrary; therefore, to facilitate interpretation of the modes, the sign of the coefficients has been reversed if required so that a positive value is always associated with a waveform with a higher peak.

All PCA, including the normalization, was performed with Matlab (MathWorks, Natick, MA, USA). The trimmed mean and mean absolute deviation were computed using the functions `trimmean(v, percent)`, which calculates the mean of a sample `v` excluding the highest and lowest (`percent`/2)% of the observations, and `mad(v)`, which computes the mean absolute deviation of `v`. PCAs were performed using the function `cpca(x, k)` from the Matlab library LIBRA[3], where `x` is the data matrix and `k` is the number of principal components to compute (Verboven and Hubert 2005).

After PCA was performed on our data, the role of each principal component was explored by plotting the average waveform plus/minus one standard deviation along the corresponding eigenmode.

Once we obtained the eigenmodes, we used them to parameterize the tests in our database. For each FMD test and for each set of eigenmodes, the first, second and third coefficients were calculated. These are the parameters that we used later in the correlations study. Potentially, it would be possible to extract these parameters from any future new FMD test performed just by calculating the coefficients of their waveforms' projections on the eigenmodes calculated from our database.

[3] Available at: http://wis.kuleuven.be/stat/robust.html.

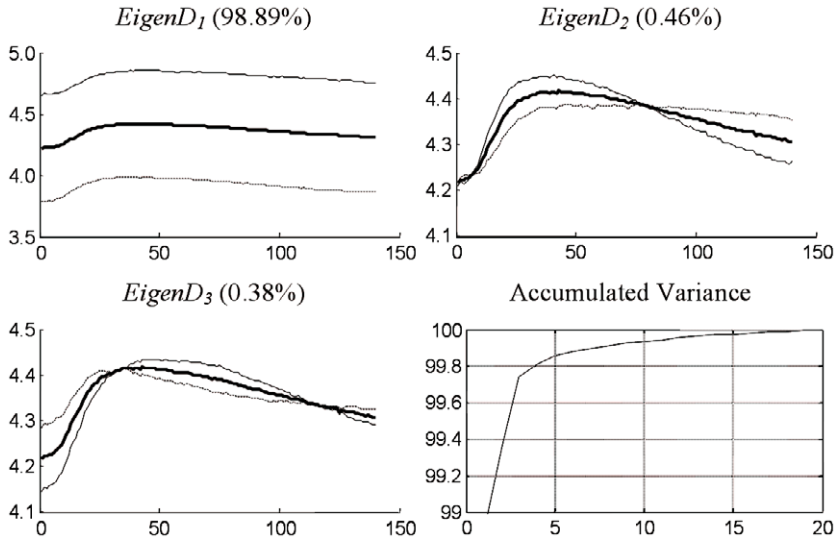

Figure 3. Representation of the variation explained by the first three *EigenD* (absolute diameter) modes. The average waveform and the waveforms resulting from the addition/subtraction of one standard deviation along the corresponding eigenmode, are plotted in bold lines and in solid/dashed lines, respectively. The *Y*-axis of each *EigenD* mode is expressed in mm. The *X*-axis represents time in s. The corresponding percentage of the total variance explained by each mode is written in parentheses in the title of each plot. The last plot shows the percentage of cumulative variance versus the number of modes taken into account. The first EigenD mode has a different scale from the other modes for purposes of visualization.

3.4. Automatic calculation of a baseline level using PCA

To compute the FMD signal (see section 3.1) for PCA we decided to use a baseline level estimate generated automatically. To this end, we used the results of PCA of the absolute diameter signal. The value at 15 s after cuff release for each waveform was reconstructed using the information recovered by the first five eigenmodes only (thus using PCA to filter out minor sources of variation), and we used this value as the baseline diameter.

4. Results: principal components analysis of FMD and velocity signals

4.1. Individual analysis of vessel size and blood velocity signals

Figures 3 and 4 show *EigenD* and *EigenFMD* modes. They correspond to the analysis of diameter and FMD data, respectively. Figure 5 shows modes from PCA of velocity data (*EigenV* modes). These three figures show the principal components of vessel size and blood velocity from the individual statistical analyses.

In order to facilitate readability of the results in the following sections, we present here a short interpretation of the changes of the waveform's morphology related to each eigenmode. This must be considered just a visual description to ease further reading, since studying the underlying physiology of eigenmodes' geometrical features is outside the scope of this work. With this caveat in mind, we could postulate that $EigenD_1$ reflects the size of the vessel, $EigenD_2$, the speed of recovery (descendent slope) combined with the height of the peak, and $EigenD_3$, the time to the peak combined with its height. $EigenFMD_1$ looks as if it reflects the scale or the size of a typical FMD waveform. $EigenFMD_2$ is very similar to $EigenD_2$; in fact, both modes show a correlation between them of $r = 0.949$. $EigenFMD_3$ reflects the time to

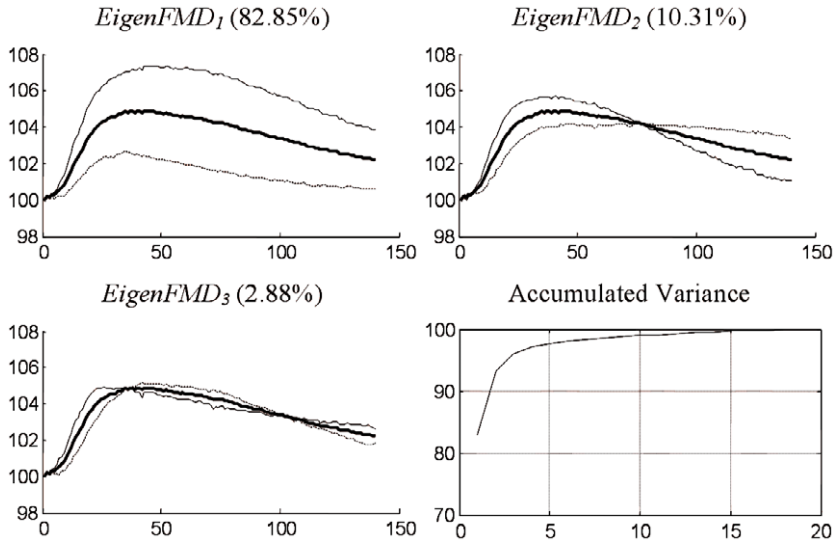

Figure 4. Representation of the variation explained by the first three EigenFMD (FMD) modes. The *Y*-axis of each *EigenFMD* mode is expressed in %FMD. See the caption in figure 3 for further explanation.

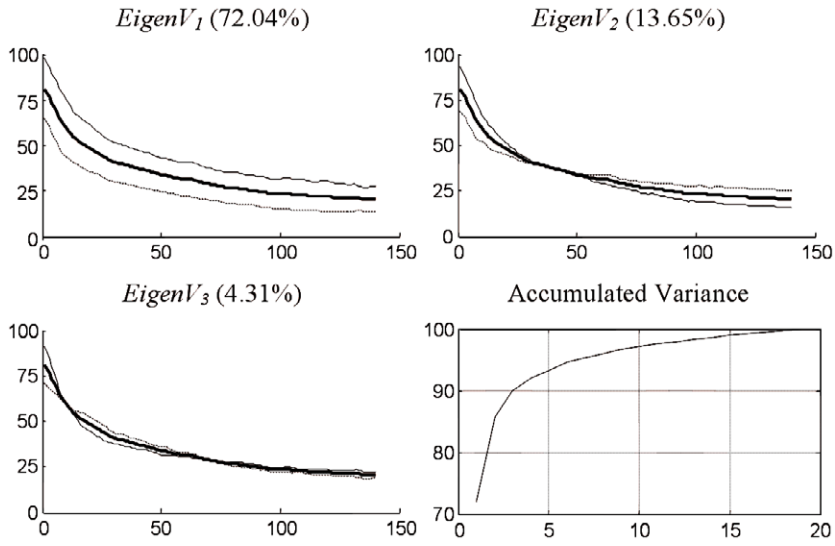

Figure 5. Representation of the variation explained by the first three *EigenV* (blood velocity) modes. The *Y*-axis of each *EigenV* mode is expressed in cm s^{-1}. See the caption in figure 3 for further explanation.

peak but independent of the height of the peak. $EigenV_1$ shows the co-variation of basal and peak blood velocity, while $EigenV_2$ indicates the variation in the peak/basal ratio.

4.2. Combined analysis of vessel size and blood velocity signals

Figures 6 and 7 show the modes from the combined statistical analysis of vessel size and blood velocity data. Figure 6 provides the results when concatenating diameter and velocity

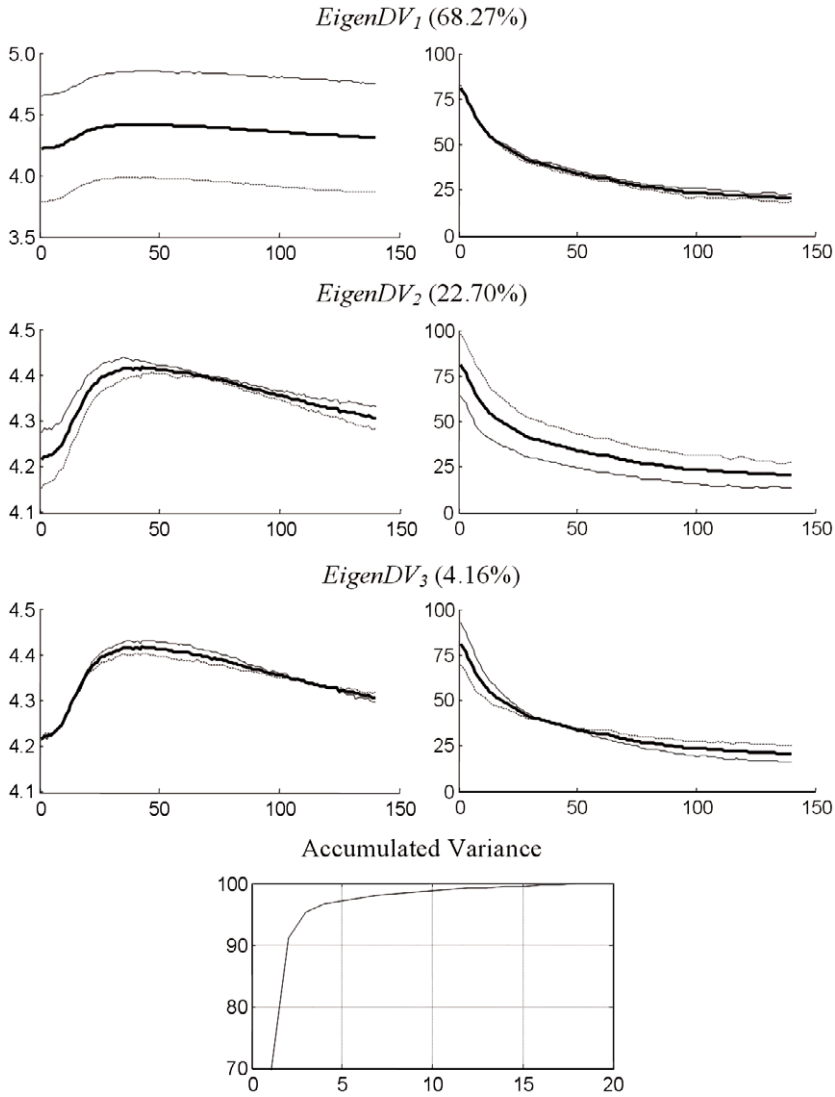

Figure 6. Representation of the variation explained by the first three combined *EigenDV* modes. See the captions in figures 3, 4 and 5 for further explanation.

segments while figure 7 does the same for FMD and velocity segments. Some conjectures about how to interpret the shape of these modes will be made next.

4.3. Correlation of PCA modes to classic FMD indices and to CVRF

The usefulness of the PCA-based parameterization was tested by checking the correlation of the eigenmodes to FMD classic indices and to clinical information, using Pearson's linear correlation coefficient. The sign of Pearson's correlation coefficient must be related to the eigenmodes' plots in figures 3–7. In order to improve readability of these results, added here is a short interpretation of the changes of the waveform's morphology as related to each eigenmode. For all analyses, statistical significance was considered reached when $p < 0.05$.

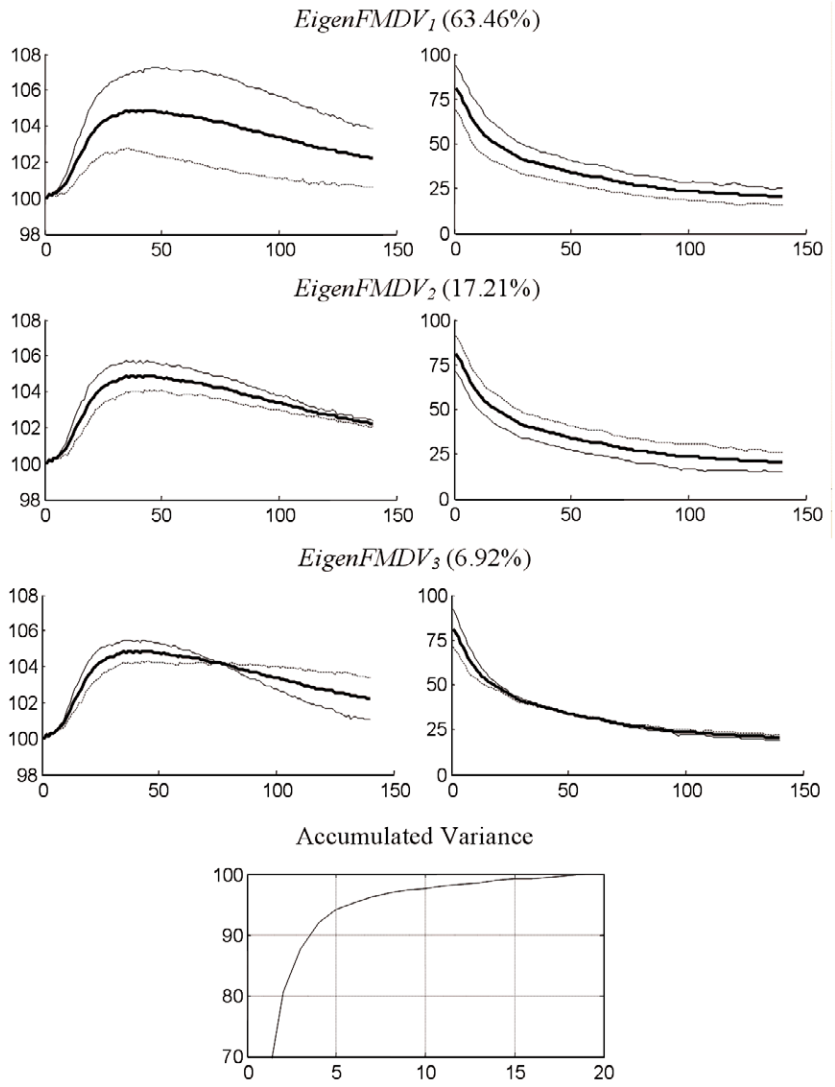

Figure 7. Representation of the variation explained by the first three combined *EigenFMDV* modes. See the captions in figures 3, 4 and 5 for further explanation.

Table 1. Pearson's correlation r coefficients (and p values) between classic parameterization and individual eigenmodes.

$n = 173$	$EigenD_1$	$EigenD_2$	$EigenD_3$	$EigenFMD_1$	$EigenFMD_2$	$EigenFMD_3$	$EigenV_1$	$EigenV_2$	$EigenV_3$
FMD_c	−0.197	+0.365	+0.782	+0.842	+0.341	−0.154	+0.394	+0.175	−0.063
	(0.009)*	(<0.001)*	(<0.001)*	(<0.001)*	(<0.001)*	(0.043)*	(<0.001)*	(0.022)*	(0.408)
$\Phi_{baseline}$	+0.986	−0.022	−0.140	−0.226	−0.290	−0.040	+0.010	−0.215	−0.022
	(<0.001)*	(0.777)	(0.066)	(0.003)*	(<0.001)*	(0.603)	(0.891)	(0.004)*	(0.774)

Statistically significant results are marked with an asterisk (*).

In tables 1 and 2, the correlations calculated between eigenmodes and classic FMD measurements are presented. Here, $\Phi_{baseline}$ was strongly correlated to $EigenD_1$ (+0.986) mode, which basically corresponds to variation in baseline diameter. The baseline estimate

Table 2. Pearson's correlation r coefficients (and p values) between classic parameterization and combined eigenmodes.

$n = 173$	$EigenDV_1$	$EigenDV_2$	$EigenDV_3$	$EigenFMDV_1$	$EigenFMDV_2$	$EigenFMDV_3$
FMD_c	−0.181	−0.425	+0.135	+0.801	+0.295	+0.270
	(0.017)*	(<0.001)*	(0.076)	(<0.001)*	(<0.001)*	(<0.001)*
$\Phi_{baseline}$	+0.981	+0.121	+0.002	−0.180	−0.238	−0.263
	(<0.001)*	(0.112)	(0.984)	(0.018)*	(0.002)*	(<0.001)*

Statistically significant results are marked with an asterisk (*).

Table 3. Pearson's correlation r coefficients (and p values) between individual eigenmodes and clinical indices.

$n = 173$	$EigenD_1$	$EigenD_2$	$EigenFMD_1$	$EigenFMD_2$	$EigenV_1$	$EigenV_2$
BMI	+0.311	+0.104	−0.066	+0.014	+0.157	−0.118
	(<0.001)*	(0.173)	(0.388)	(0.857)	(0.040)*	(0.124)
HDL-C	−0.167	+0.091	−0.012	+0.127	−0.144	+0.106
	(0.028)*	(0.237)	(0.879)	(0.096)	(0.060)	(0.166)
LDL-C	+0.052	−0.244	−0.114	−0.243	−0.044	−0.129
	(0.499)	(0.001)*	(0.139)	(0.001)*	(0.564)	(0.092)
Trig	+0.242	+0.057	+0.052	−0.008	+0.091	+0.025
	(0.001)*	(0.457)	(0.496)	(0.918)	(0.236)	(0.744)

BMI = body mass index. HDL-C = HDL-Cholesterol. LDL-C = LDL-Cholesterol. Trig = Triglycerides. Statistically significant results are marked with an asterisk (*).

described in section 3.3 also showed a high correlation with $\Phi_{baseline}$ (+0.980). This classic measure correlated as well with $EigenFMD_1$, $EigenFMD_2$, $EigenV_2$, $EigenDV_1$ (+0.981), and the first three modes of $EigenFMDV$. Moving on to FMD_c, we observed that it was correlated mainly to $EigenFMD_1$ and to $EigenD_3$ (+0.842 and +0.782, respectively), consistent with higher dilations. This is not surprising since $EigenFMD_1$ represents variation of some sort of 'scale or size of the curve' and $EigenD_3$ represents height of peak dilation associated with the timing of the peak (the higher the peak, the later the maximum, and vice versa). FMD_c was also significantly correlated to all other modes tested in tables 1 and 2 except to $EigenV_3$ and $EigenDV_3$.

In table 3, the coefficients of correlation between clinical information and individual eigenmodes are presented. A correlation was found between $EigenD_1$ and BMI (+0.311), HDL-Cholesterol (−0.167), and Triglycerides (+0.242). The strengths of these correlations are similar to those found for the baseline diameter and these clinical parameters. $EigenD_2$ adds more information, as it correlates negatively (−0.244) to LDL-Cholesterol, just as $EigenFMD_2$, which has a similar shape. This relationship means that higher dilations and quicker recovery slopes after peak line up with lower LDL-Cholesterol levels. Conversely, no significant correlation was found for $EigenFMD_1$.

Pearson's coefficients of linear correlation between combined eigenmodes and clinical parameters are shown in table 4. Among $EigenDV$ modes, $EigenDV_1$ is the only mode that correlates with risk factors and it does so in a very similar way to $EigenD_1$. Probably the intense variation of baseline diameter independent of blood velocity prevents other modes from presenting relevant information. None of the correlations found for $EigenFMDV_1$ and clinical parameters was statistically significant. This is not surprising, given that this mode seems to be comprised of the combination of $EigenFMD_1$ and $EigenV_1$ with proportional variation, and no significant correlation was found for any of these individual modes. On the other hand, $EigenFMDV_2$ correlates with BMI (−0.230) and HDL-Cholesterol (+0.164). This mode represents variation in peak dilation moving in an opposite direction to the peak

Table 4. Pearson's correlation r coefficients (and p values) between combined eigenmodes and clinical indices.

$n = 173$	$EigenDV_1$	$EigenDV_2$	$EigenDV_3$	$EigenFMDV_1$	$EigenFMDV_2$	$EigenFMDV_3$
BMI	+0.317	−0.114	−0.052	−0.008	−0.230	+0.045
	(<0.001)*	(0.135)	(0.494)	(0.919)	(0.002)*	(0.562)
HDL-C	−0.174	+0.121	+0.076	−0.052	+0.164	+0.108
	(0.023)*	(0.114)	(0.323)	(0.497)	(0.032)*	(0.159)
LDL-C	+0.052	+0.052	−0.122	−0.106	−0.080	−0.238
	(0.503)	(0.498)	(0.113)	(0.170)	(0.299)	(0.002)*
Trig	+0.244	−0.060	+0.080	+0.070	−0.058	+0.023
	(0.001)*	(0.437)	(0.294)	(0.361)	(0.450)	(0.765)

BMI = body mass index. HDL-C = HDL-Cholesterol. LDL-C = LDL-Cholesterol. Trig = Triglycerides. Statistically significant results are marked with an asterisk (*).

Table 5. Pearson's correlation r coefficients (and p values) between classic parameterization and clinical indices.

$n = 173$	$\Phi_{baseline}$	BMI	LDL-C	HDL-C	Trig.
FMD_c	−0.351	−0.095	−0.177	+0.090	+0.021
	(<0.001)*	(0.217)	(0.021)*	(0.238)	(0.785)
$\Phi_{baseline}$		+0.315	+0.068	−0.174	+0.230
		(<0.001)*	(0.379)	(0.022)*	(0.002)*

BMI = body mass index. HDL-C = HDL-Cholesterol. LDL-C = LDL-Cholesterol. Trig = Triglycerides. Statistically significant results are marked with an asterisk (*).

blood velocity (the lower the velocity, the higher the vasodilation); i.e., high HDL-Cholesterol levels are associated with high dilation and lower peak blood velocity, and in contrast, higher BMI is associated with the inverse behaviour. Finally, $EigenFMDV_3$ is correlated with LDL-Cholesterol (−0.238). Lower peak blood velocity with lower dilation and slower recovery of baseline levels are associated with higher levels of LDL-Cholesterol.

For comparison purposes, table 5 shows the correlations between classic measurements of FMD waveforms and clinical information in our sample.

5. Discussion

This paper presents a methodology for a detailed parameterization and analysis of the time course of FMD and blood velocity signals based on PCA. Any signal from new FMD tests performed can be decomposed this way, just by calculating the coefficients of their projections on the eigenmodes derived from our database, thus providing the descriptive parameters that we have shown.

The parameters extracted by PCA of both FMD and diameter signals were consistent with classic indices. $EigenFMD_1$ and $EigenD_3$, which include peak dilation as an important component of their variation, showed the highest correlation with classic peak dilation, although most of other modes also correlated with it. Additionally, $EigenD_1$ was strongly correlated to baseline diameter. Furthermore, we showed that PCA allows objective estimates of baseline diameter.

We selected serum lipids as prototypical CVRF and compared classic versus new parameterization in detecting the relationship between lipids and endothelial function. It has been shown in the literature that serum lipids, in particular total cholesterol and LDL-Cholesterol, are main causal factors of atherosclerosis while HDL-Cholesterol is a protective

factor (NCEP-ATP III (NCEP 2001)). This pathology is caused by accumulation of lipids in the vessel wall, which finally compromises the basic vascular function to distribute sufficient blood flow to the affected areas. Higher total cholesterol and LDL-Cholesterol levels are supposed to increase cardiovascular risk by impairing endothelial function (Clarkson *et al* 1996). On the other hand, recent studies suggest that high HDL-Cholesterol clearly benefits the vascular endothelium (Zhang *et al* 2000, Toikka *et al* 1999, Kuvin *et al* 2003, Lupattelli *et al* 2002).

Table 5 shows the correlations that we found between classic FMD measurements and clinical information in our sample. It is not the first time that this relationship has been studied (Zhang *et al* 2000, Lupattelli *et al* 2002, 2000, Brook *et al* 2001, Malik *et al* 2001, Li *et al* 2000, Aggoun *et al* 2000, Sorensen *et al* 1994, Vaudo *et al* 2003, Ravikumar *et al* 2002, Jensen-Urstad *et al* 1997, Schroeder *et al* 2000, Jensen-Urstad *et al* 1999, Paivansalo *et al* 2000). Baseline diameter positively correlated with BMI and Triglycerides and negatively with HDL-Cholesterol in our sample, in agreement with what was also reported in other studies (Jensen-Urstad *et al* 1997, 1999, Paivansalo *et al* 2000). Classic FMD_c was negatively correlated to LDL-Cholesterol (-0.180) in our sample, implying that higher LDL-Cholesterol levels are linked to lower peak dilations, a fact that was also found in Lupattelli *et al* (2002) (-0.290), Li *et al* (2000) (-0.237) and Aggoun *et al* (2000) (-0.400). No other associations were found for FMD_c in this particular sample. Nonetheless, significant positive (protective) correlations have been described between HDL-Cholesterol and FMD_c (coefficients ranging from 0.220 to 0.590) (Zhang *et al* 2000, Lupattelli *et al* 2002, 2000, Li *et al* 2000, Vaudo *et al* 2003, Jensen-Urstad *et al* 1997), and negative (damaging) correlations between Triglycerides and FMD_c (coefficients ranging from -0.380 (Vaudo *et al* 2003) to -0.760 (Lupattelli *et al* 2000)). In the literature, it is somewhat difficult to find reports of these correlations, and results are heterogeneous since extreme values of risk factors have a small representation in natural samples like ours. Usually pooled samples that combine two risk levels are used to artificially increase the detected association strength (Zhang *et al* 2000, Lupattelli *et al* 2000, Li *et al* 2000, Sorensen *et al* 1994, Ravikumar *et al* 2002). Also, some studies are carried out on diseased groups (Lupattelli *et al* 2002, Malik *et al* 2001, Aggoun *et al* 2000). Nevertheless, despite the different correlation strengths and success in finding statistical significance in the literature, all of the aforementioned reports, including our own classic indices calculations, show correlations with consistent direction.

With regard to the relationship between variables within the FMD test, a negative correlation between FMD_c and baseline diameter was also found (-0.333) in our sample, meaning that wider arteries tend to dilate less (also a known fact (Zhang *et al* 2000)), highlighting the link between artery diameter and FMD that justifies the dual (diameter and FMD signals) approach (Li *et al* 2000, Schroeder *et al* 2000, Jensen-Urstad *et al* 1999).

With respect to the new parameters, we verified that some of them correlated with serum lipids. It is worth noting that each clinical factor was related to a different set of parameters. Considering that the different eigenmodes can be related to different descriptive features of the FMD process such as maximum peak, mean level, time to peak, recovery speed or dynamic range, we can infer that the different lipids tested do not exhibit a homogeneous association with the different morphological features of the FMD waveform. Therefore, our parameterization provides more comprehensive information than classic indices, thus allowing a more detailed description of the FMD process. Reinforcing the validity of our findings, the associations found between individual eigenmodes and risk factors were consistent with what the classic analysis found in our sample and with other reports in the clinical literature. Moreover, these parameters tend to show a stronger association with the lipids tested than classic FMD_c and $\Phi_{baseline}$, suggesting that parameterization of FMD by PCA is more sensitive to clinical

variables and CVRF than classic indices. Further, some of the modes are more specific to particular disorders than the more generic FMD_c. For example, correlations of $EigenD_2$ and $EigenFMD_2$ with LDL-Cholesterol seem stronger (-0.244 and -0.243) than the correlation presented by the classic index FMD_c (-0.177). These modes apparently reflect the velocity of decay and the peak height.

The eigenmodes of the combined statistical analysis summarize some aspects of the interplay between FMD and blood velocity, or diameter and blood velocity, thus allowing for a clearer distinction between the different effects that modify the vasodilatory response. Interestingly, $EigenFMDV_1$ represents a collinear variation of peak blood velocity and dilation, and none of the risk factors correlated significantly with this mode. Indeed, in this mode, the vasodilation is directly proportional to the peak blood velocity stimulus. Therefore, we could hypothesize that this mode may model the system response to reactive hyperaemia (the higher the peak blood velocity, the larger the vasodilation), given the different hyperaemic responses in the sample. In contrast, $EigenFMDV_2$ represents variations in opposite directions of the peak blood velocity and of the peak dilation. In this mode, an increase in peak blood velocity corresponds to a decrease in FMD peak level, probably reflecting cases in which even greater blood velocity impulses are not enough to produce a normal dilation. This desensitization of the endothelium to the stimulus appears to be associated with low HDL-Cholesterol and high BMI. It seems logical that the presence of higher velocity impulses provoking less dilation indicates impairment of the system, probably due to a damaged endothelium. Again, PCA proved to grant a more detailed description of FMD than the classic measurement.

Future work on the flow mediated dilation mechanics could consider the shear stress signal instead of blood velocity, which is used as a surrogate. The former is modified by some variables that change across the cardiac cycle and across the FMD test. To get a good estimate of shear stress, instantaneous blood velocity, diameter and sectional velocity profile should be considered and their changes in time taken into account. Ideally, a direct measurement would be preferable to a mathematical convolution of these signals, to preserve independence towards statistical analysis. We just used the time-averaged maximum velocity across the cardiac cycle and consequently, our statistical conclusions are referred to as blood velocity and not as shear stress.

PCA is probably also a suitable statistical tool for decomposing other time-based signals used to study the endothelium in other types of vascular tests. Laser Doppler provides such signals for post-occlusive reactive hyperaemia in human forearm skin tests or for iontophoresis of acetylcholine tests. Also, digital reactive hyperaemia by peripheral arterial tonometry is evaluated by analysing a time-based signal. Nevertheless, these techniques only evaluate flow changes and the endothelial reactivity of microcirculation. In contrast, FMD evaluates both, diameter changes due to responses of conduit arteries and the post-occlusive reactive hyperaemia, which is due to responses in the microcirculation. In any case, detailed parameterization of results in those tests might also provide insight into these complex endothelial processes.

6. Summary and conclusions

In this paper, we introduced a novel parameterization of vasodilation and blood velocity signals from flow-mediated dilation tests through principal component analysis (PCA). We analysed FMD tests from a sample of healthy men. The signals were extracted from ultrasound image sequences of the brachial artery using computerized measurement techniques, which have already been published. From the analysis, several principal components or eigenmodes could

be determined. Each eigenmode seemed, through visual inspection, related to different aspects of the morphology of the waveforms.

The eigenmodes were used to obtain a global parameterization of diameter, FMD and velocity signals. The parameters correlated with classic measurements on FMD tests. They also were able to capture relationships between FMD and plasma lipids, such as the inverse roles HDL-Cholesterol and LDL-Cholesterol have in endothelial function, showing plausible correlations in accordance with reports in the clinical literature. Moreover, some of these associations showed higher strength than those found for traditional parameters and lipids. Furthermore, FMD was decomposed in several uncorrelated components, allowing a more detailed analysis than before: we could detect that each cholesterol fraction was associated with a different mode. In addition, we proved that PCA parameterization of absolute diameter waveform can be used to get an objective estimate of baseline diameter. Our work opens new possibilities for interpreting FMD tests: using the eigenmodes derived from our database as reference, it will be possible to obtain these parameters for FMD tests performed on other new subjects, especially considering that the presented parameterization can be used either with our computerized analysis of ultrasound images or in combination with other computerized approaches as found in the literature.

At the same time, we investigated the mutual relationship between FMD and velocity waveforms through a combined statistical analysis. The first principal component, bearing most of the signal variability, did not correlate to the CVRF that we tested and it seemed to capture mostly the linear relationship between the flow stimulus and the vasodilatory response; another mode reflected smaller responses of the conduit artery endothelium to the flow stimulus, which we found to be associated with low HDL-Cholesterol; and a third mode described a decreased flow stimulus and decelerated recovery of the baseline, which was associated with high LDL-Cholesterol. The combined analysis of dilation and velocity signals paves the way for a new insight into the interpretation of FMD tests.

In conclusion, the global parameterization that we proposed has proven its applicability as a detailed statistical analysis of the dynamics of the vasodilation process and its link to CVRF.

Acknowledgments

This work was partially supported by MEC TEC2006-03617, and ISCIII G03/185, CB06/01/0061, FIS2004/40676 and FIS1999/600 grant. The work of M Laclaustra is supported by the Spanish Ministry of Health and Consumption under a FIS Fellowship from the Instituto de Salud 'Carlos III'. The work of A.G Frangi was supported by the Aragon Government under a FPI Grant B197/2003. The work of L Boisrobert is supported by the Spanish Ministry of Education and Science under a FPU Grant AP-2002-3946. The work of A F Frangi is supported by the Spanish Ministry of Education and Science under a Ramón y Cajal Research Fellowship.

Appendix A. Overview of the method for obtaining the diameter signal from ultrasound image sequences

The method introduced in Frangi *et al* (2003) has been used to detect diameter changes across time from ultrasound image sequences. In contrast to other methods based on dynamic programming, deformable models (Fan *et al* 2000, 2001, Sonka *et al* 2002, Liang *et al* 2000, Preik *et al* 2000, Woodman *et al* 2001) or neural networks (Newey and Nassiri 2002), which

perform edge detection, this method is based on a global image registration strategy to quantify flow-mediated vasodilation. Inter-frame arterial changes are modelled as a superposition of a rigid motion (translation and rotation) and a scaling factor normal to the artery. Every frame in the ultrasound sequence is compared to a reference frame and the registration algorithm estimates the transversal deformation of the artery with respect to that frame.

The method has been programmed in C++ and currently runs in the PC environment. It requires minimum skills and no training to be used; therefore, results are scarcely operator dependent. Our internal quality tests performed on the sequences used for this study yielded an error with a standard deviation of 1.17 units of artery dilation, a value that even exceeds the accuracy published in the first validation of the technique (Frangi *et al* 2003). This value is smaller than half of the error of an expert manual reader and better than error values reported for other automated methods previously published. Furthermore, lower image quality did not substantially compromise accuracy, contrary to what happens with other methods (manual or automatic) that rely on edge detection. In Frangi *et al* (2003), image samples of different quality within the database can be seen. Thanks to this method, FMD tests can be reliably performed without the absolute requirement of expensive high-frequency ultrasound probes.

Our method directly provides a signal holding the evolution of vasodilation relative to the reference frame (automated relative signal). In our study, this reference frame was selected at 60 s after release of the cuff, which approximately coincides with the peak of FMD.

The absolute diameter signal was obtained by multiplying the automated relative signal by a diameter manually assessed in the reference frame. Manual measurements were obtained by fitting spline curves to the inner contours of the media layer of the near and far arterial walls. Diameters are computed from the average distance between the two lines. For further details of the manual measurement protocol, please refer to appendix II in Frangi *et al* (2003). Manual measurements are accurate enough (standard deviation of the error is approximately 100 μm) to detect inter-subject diameter differences (range in our sample 3043–5395 μm), which is the purpose for their being used here.

We chose to follow the described procedure, but note that obtaining the absolute diameter signal (thus manually measuring the diameter of the reference frame) is not mandatory to obtain FMD_c measurements (see section 3.1). This is also the case for computing the FMD signal (see section 3.1). The automated relative signal, the FMD signal and the diameter signal are all scaled versions of one another and equation (1) is valid for all of them. The scaling factor that links and differentiates the signals cancels itself out by being present in both sides of the fraction. Thus, FMD_c and the FMD signal could have been calculated directly from the automated relative signal just by manually reading the baseline and maximum levels (figures 1 and 2).

Appendix B. Overview of the method for obtaining the blood velocity signal from ultrasound image sequences

Blood velocity is quantified by automatic segmentation of the Doppler ultrasound blood velocity spectral waveforms present in the digitized image frames. The automated technique that we used to analyse each frame resembles the method presented by Tschirren *et al* (2001). Overall, the main differences in our case were that less noise filtering was required; that segmentation of the velocity spectral waveform from the digitized screen was performed column-wise (i.e. time-wise) instead of performing a bi-dimensional segmentation; and that our identification of each cardiac cycle was directly provided by the ultrasound system instead of being inferred from the shape of the chart. Briefly, the steps were the following: detection of the horizontal axis; extraction of the envelope of the blood velocity spectrum by image

thresholding and edge detection (time-wise); separation of individual cardiac cycles within this maximum blood velocity curve (in each frame two or more cardiac cycles are depicted); and averaging of blood velocity of the most recent cycle present in the image. Velocity signal contained the time-averaged maximum velocity information for the last beat depicted on each frame in the sequence. Occasionally, in some isolated frames it was not possible to recover the velocity information because of synchronization problems and, in these cases, the missing velocity sample was filled in from its adjacent samples using cubic interpolation. The impact of inferring those isolated gaps in our results is minimal if one takes into account that interpolation is only seldom used and that the velocity change rate is very slow (changes occur in several seconds) compared to the sampling frequency of the velocity signal (1 Hz).

References

Aggoun Y, Bonnet D, Sidi D, Girardet J P, Brucker E, Polak M, Safar M E and Levy B I 2000 Arterial mechanical changes in children with familial hypercholesterolemia *Arterioscler. Thromb. Vasc. Biol.* **20** 2070–5

Brook R D, Bard R L, Rubenfire M, Ridker P M and Rajagopalan S 2001 Usefulness of visceral obesity (waist/hip ratio) in predicting vascular endothelial function in healthy overweight adults *Am. J. Cardiol.* **88** 1264–9

Casasnovas J A, Lapetra A, Puzo J, Pelegrin J, Hermosilla T, De Vicente J, Garza F, Del Rio A, Giner A and Ferreira I J 1992 Tobacco, physical exercise and lipid profile *Eur. Heart J.* **13** 440–5

Celermajer D S, Sorensen K E, Georgakopoulos D, Bull C, Thomas O, Robinson J and Deanfield J E 1993a Cigarette smoking is associated with dose-related and potentially reversible impairment of endothelium-dependent dilation in healthy young adults *Circulation* **88** 2149–55

Celermajer D S, Sorensen K E, Gooch V M, Spiegelhalter D J, Miller O I, Sullivan I D, Lloyd J K and Deanfield J E 1992 Non-invasive detection of endothelial dysfunction in children and adults at risk of atherosclerosis *Lancet* **340** 1111–5

Celermajer D S, Sorensen K, Ryalls M, Robinson J, Thomas O, Leonard J V and Deanfield J E 1993b Impaired endothelial function occurs in the systemic arteries of children with homozygous homocystinuria but not in their heterozygous parents *J. Am. Coll. Cardiol.* **22** 854–8

Clarkson P, Celermajer D S, Donald A E, Sampson M, Sorensen K E, Adams M, Yue D K, Betteridge D J and Deanfield J E 1996 Impaired vascular reactivity in insulin-dependent diabetes mellitus is related to disease duration and low density lipoprotein cholesterol levels *J. Am. Coll. Cardiol.* **28** 573–9

Cooke J P, Rossitch E Jr, Andon N A, Loscalzo J and Dzau V J 1991 Flow activates an endothelial potassium channel to release an endogenous nitrovasodilator *J. Clin. Invest.* **88** 1663–71

Corretti M C *et al* 2002 Guidelines for the ultrasound assessment of endothelial-dependent flow-mediated vasodilation of the brachial artery: a report of the International Brachial Artery Reactivity Task Force *J. Am. Coll. Cardiol.* **39** 257–65

Fan L, Santago P, Jiang H and Herrington D M 2000 Ultrasound measurement of brachial flow-mediated vasodilator response *IEEE Trans. Med. Imaging* **19** 621–31

Fan L, Santago P, Riley W and Herrington D M 2001 An adaptive template-matching method and its application to the boundary detection of brachial artery ultrasound scans *Ultrasound Med. Biol.* **27** 399–408

Faulx M D, Wright A T and Hoit B D 2003 Detection of endothelial dysfunction with brachial artery ultrasound scanning *Am. Heart J.* **145** 943–51

Frangi A F, Laclaustra M and Lamata P 2003 A registration-based approach to quantify flow-mediated dilation (FMD) of the brachial artery in ultrasound image sequences *IEEE Trans. Med. Imaging* **22** 1458–69

Gokce N, Keaney J F Jr, Hunter L M, Watkins M T, Nedeljkovic Z S, Menzoian J O and Vita J A 2003 Predictive value of noninvasively determined endothelial dysfunction for long-term cardiovascular events in patients with peripheral vascular disease *J. Am. Coll. Cardiol.* **41** 1769–75

Hardie K L, Kinlay S, Hardy D B, Wlodarczyk J, Silberberg J S and Fletcher P J 1997 Reproducibility of brachial ultrasonography and flow-mediated dilatation (FMD) for assessing endothelial function *Aust. N Z J. Med.* **27** 649–52

Jensen-Urstad K, Jensen-Urstad M and Johansson J 1999 Carotid artery diameter correlates with risk factors for cardiovascular disease in a population of 55-year-old subjects *Stroke* **30** 1572–6

Jensen-Urstad K, Johansson J and Jensen-Urstad M 1997 Vascular function correlates with risk factors for cardiovascular disease in a healthy population of 35-year-old subjects *J. Int. Med.* **241** 507–13

Jolliffe I T 2002 *Principal Component Analysis* 2nd edn (New York: Springer) (Springer Series in Statistics)

Kuvin J T, Patel A R, Sidhu M, Rand W M, Sliney K A, Pandian N G and Karas R H 2003 Relation between high-density lipoprotein cholesterol and peripheral vasomotor function *Am. J. Cardiol.* **92** 275–9

Laclaustra-Gimeno M, Gonzalez-Garcia M P, Casasnovas-Lenguas J A, Luengo-Fernandez E, Leon-Latre M, Portero-Perez P, Del Rio-Ligorit A, Giner-Soria A and Ferreira-Montero I J 2006 Cardiovascular risk factor progression in young males at 15-year follow-up in the General Military Academy of Zaragoza (AGEMZA) Study *Rev. Esp. Cardiol.* **59** 671–8

Li X P, Zhao S P, Zhang X Y, Liu L, Gao M and Zhou Q C 2000 Protective effect of high density lipoprotein on endothelium-dependent vasodilatation *Int. J. Cardiol.* **73** 231–6

Liang Q, Wendelhag I, Wikstrand J and Gustavsson T 2000 A multiscale dynamic programming procedure for boundary detection in ultrasonic artery images *IEEE Trans. Med. Imaging* **19** 127–42

Lupattelli G, Lombardini R, Schillaci G, Ciuffetti G, Marchesi S, Siepi D and Mannarino E 2000 Flow-mediated vasoactivity and circulating adhesion molecules in hypertriglyceridemia: association with small, dense LDL cholesterol particles *Am. Heart J.* **140** 521–6

Lupattelli G, Marchesi S, Roscini A R, Siepi D, Gemelli F, Pirro M, Sinzinger H, Schillaci G and Mannarino E 2002 Direct association between high-density lipoprotein cholesterol and endothelial function in hyperlipemia *Am. J. Cardiol.* **90** 648–50

Malik J, Melenovsky V, Wichterle D, Haas T, Simek J, Ceska R and Hradec J 2001 Both fenofibrate and atorvastatin improve vascular reactivity in combined hyperlipidaemia (fenofibrate versus atorvastatin trial–FAT) *Cardiovasc. Res.* **52** 290–8

Moncada S and Higgs A 1993 The L-arginine-nitric oxide pathway *N. Engl. J. Med.* **329** 2002–12

NCEP Executive Summary of The Third Report of The National Cholesterol Education Program 2001 Expert panel on detection, evaluation, and treatment of high blood cholesterol in adults (adult treatment panel III) *JAMA* **285** 2486–97

Newey V R and Nassiri D K 2002 Online artery diameter measurement in ultrasound images using artificial neural networks *Ultrasound Med. Biol.* **28** 209–16

Paivansalo M J, Merikanto J, Jerkkola T, Savolainen M J, Rantala A O, Kauma H, Lilja M, Reunanen Y A, Kesaniemi A and Suramo I 2000 Effect of hypertension and risk factors on diameters of abdominal aorta and common iliac and femoral arteries in middle-aged hypertensive and control subjects: a cross-sectional systematic study with duplex ultrasound *Atherosclerosis* **153** 99–106

Preik M, Lauer T, Heiss C, Tabery S, Strauer B E and Kelm M 2000 Automated ultrasonic measurement of human arteries for the determination of endothelial function *Ultraschall. Med.* **21** 195–8

Ravikumar R, Deepa R, Shanthirani C and Mohan V 2002 Comparison of carotid intima-media thickness, arterial stiffness, and brachial artery flow mediated dilatation in diabetic and nondiabetic subjects (The Chennai Urban Population Study) *Am. J. Cardiol.* **90** 702–7

Roberts W C 1988 The Friedewald–Levy–Fredrickson formula for calculating low-density lipoprotein cholesterol, the basis for lipid-lowering therapy *Am. J. Cardiol.* **62** 345–6

Schroeder S, Enderle M D, Baumbach A, Ossen R, Herdeg C, Kuettner A and Karsch K R 2000 Influence of vessel size, age and body mass index on the flow-mediated dilatation (FMD%) of the brachial artery *Int. J. Cardiol.* **76** 219–25

Silber H A, Bluemke D A, Ouyang P, Du Y P, Post W S and Lima J A 2001 The relationship between vascular wall shear stress and flow-mediated dilation: endothelial function assessed by phase-contrast magnetic resonance angiography *J. Am. Coll. Cardiol.* **38** 1859–65

Silber H A, Ouyang P, Bluemke D A, Gupta S N, Foo T K and Lima J A 2005 Why is flow-mediated dilation dependent on arterial size? Assessment of the shear stimulus using phase-contrast magnetic resonance imaging *Am. J. Physiol. Heart. Circ. Physiol.* **288** H822–8

Sinoway L I, Hendrickson C, Davidson W R Jr, Prophet S and Zelis R 1989 Characteristics of flow-mediated brachial artery vasodilation in human subjects *Circ. Res.* **64** 32–42

Sonka M, Liang W and Lauer R M 2002 Automated analysis of brachial ultrasound image sequences: early detection of cardiovascular disease via surrogates of endothelial function *IEEE Trans. Med. Imaging* **21** 1271–9

Sorensen K E, Celermajer D S, Georgakopoulos D, Hatcher G, Betteridge D J and Deanfield J E 1994 Impairment of endothelium-dependent dilation is an early event in children with familial hypercholesterolemia and is related to the lipoprotein(a) level *J. Clin. Invest.* **93** 50–5

Teragawa H, Kato M, Kurokawa J, Yamagata T, Matsuura H and Chayama K 2001 Usefulness of flow-mediated dilation of the brachial artery and/or the intima-media thickness of the carotid artery in predicting coronary narrowing in patients suspected of having coronary artery disease *Am. J. Cardiol.* **88** 1147–51

Toikka J O, Ahotupa M, Viikari J S, Niinikoski H, Taskinen M, Irjala K, Hartiala J J and Raitakari O T 1999 Constantly low HDL-cholesterol concentration relates to endothelial dysfunction and increased in vivo LDL-oxidation in healthy young men *Atherosclerosis* **147** 133–8

Tschirren J, Lauer R M and Sonka M 2001 Automated analysis of Doppler ultrasound velocity flow diagrams *IEEE Trans. Med. Imaging* **20** 1422–5

Vaudo G, Marchesi S, Lupattelli G, Pirro M, Pasqualini L, Roscini A R, Siepi D, Schillaci G and Mannarino E 2003 Early vascular damage in primary hypoalphalipoproteinemia *Metabolism* **52** 328–32

Verboven S and Hubert M 2005 Libra: a Matlab Library for Robust Analysis *Chemometr. Intell. Lab. Syst.* **75** 127–36

Vita J A and Keaney J F Jr 2002 Endothelial function: a barometer for cardiovascular risk? *Circulation* **106** 640–2

Widlansky M E, Gokce N, Keaney J F Jr and Vita J A 2003 The clinical implications of endothelial dysfunction *J. Am. Coll. Cardiol.* **42** 1149–60

Woodman R J *et al* 2001 Improved analysis of brachial artery ultrasound using a novel edge-detection software system *J. Appl. Physiol.* **91** 929–37

Zhang X, Zhao S P, Li X P, Gao M and Zhou Q C 2000 Endothelium-dependent and-independent functions are impaired in patients with coronary heart disease *Atherosclerosis* **149** 19–24